Polymer 50 (2009) 585–590

Contents lists available at ScienceDirect

Polymer

journal homepage: www.elsevier.com/locate/polymer

Yielding in ethylene/methacrylic acid ionomers

Robert C. Scogna, Richard A. Register*

Department of Chemical Engineering, Princeton University, Princeton, NJ 08544-5263, United States

ARTICLE INFO

Article history:
Received 19 October 2008
Received in revised form
30 November 2008
Accepted 2 December 2008
Available online 9 December 2008

Keywords:
Ethylene copolymer
Ionomer
Yield stress

ABSTRACT

Ethylene/methacrylic acid (E/MAA) ionomers exhibit a complex morphology – consisting of polyethylene crystals, amorphous polymer segments and ionic aggregates – as well as pronounced differences in mechanical properties compared with the E/MAA copolymers from which they are derived. Here, we illuminate the microstructural origins of the changes in one such property – the yield stress – imparted to E/MAA by partial neutralization with sodium. The yield stress reflects contributions from both polyethylene crystal plasticity and incomplete mechanical relaxation of the ion-containing amorphous phase; the amorphous phase, in turn, consists of ion-rich aggregates and ion-poor domains, with widely separated relaxation rates. The inability of the amorphous material immediately surrounding the ionic aggregates to relax, except at extremely low strain rates, greatly increases the yield stress of the ionomers. Only a minor fraction of the E/MAA groups must be neutralized to create ion-rich aggregates, and thus to achieve the limiting yield stress behavior. The slow growth of thin polyethylene crystals also has a marked influence; as they form after quenching from the melt, these secondary crystals bridge the gaps between the locally-vitrified amorphous regions, leading to a large increase in yield stress.

1. Introduction

Ionomers are polymers that bear a small fraction of ionic functional groups pendant to the polymer backbone [1]. One particularly useful class of ionomers is derived from partial or complete neutralization of the acid moieties in a semicrystalline ethylene/methacrylic acid copolymer (E/MAA) with a metal cation such as sodium, magnesium or zinc. The resulting ionomer is exceptionally tough [2] and typically used as a cut- and scratch-resistant coating or puncture-resistant film packaging [3]. Despite more than four decades of widespread commercial use, rather little work has been done [4–6] to determine which mechanisms are responsible for the desirable mechanical properties.

On the other hand, a thorough investigation of the yield behavior of the unneutralized E/MAA copolymers was recently presented [7]. The yield stress (σ_y) of these resins was well described by a simple superposition of contributions from polyethylene crystal plasticity and incomplete amorphous relaxation. A strain rate–temperature superposition algorithm was developed which allowed for the creation of yield stress master curves. It was shown that the yield stress of these copolymers at room temperature is highly dependent upon the glass transition temperature (T_g), which is a function of MAA content. For high-MAA-content copolymers, T_g can exceed room temperature. The resulting vitrification of the amorphous phase results in an increase in the yield stress, despite the reduction in degree of crystallinity with higher MAA content.

The aim of this work is to investigate how the yield stress changes upon "ionomerization" – partial neutralization of the MAA groups, in this case with sodium. Up to a critical degree of neutralization of 0.4 wt% Na, we find a several-fold increase in σ_y at typical laboratory strain rates; further neutralization results in minimal gains. The elevation of σ_y is attributed to the incomplete relaxation of polymer chain segments within the "regions of restricted mobility", as termed by Eisenberg et al. [8]. Incomplete relaxation of stress within these regions of restricted mobility increases both the stiffness and the ability to withstand plastic deformation. Finally, the slow growth of thin secondary crystals in the amorphous regions of the ionomers serves to reinforce the influence of these regions of restricted mobility by tying them together [9].

2. Experimental section

2.1. Materials

E/MAA copolymers and ionomers were provided by DuPont Packaging and Industrial Polymers. The acid copolymers (base

* Corresponding author. Department of Chemical Engineering, Princeton University, A217 Engineering Quadrangle, Princeton, NJ 08544-5263, United States. Tel.: +1 609 258 4691; fax: +1 609 258 0211.
E-mail address: register@princeton.edu (R.A. Register).

0032-3861/$ – see front matter © 2008 Elsevier Ltd. All rights reserved.
doi:10.1016/j.polymer.2008.12.003

resins) contained 11.5, 15 and 19 wt% MAA (4.1, 5.5 and 7.1 mol% MAA), with melt indices (ASTM D1238 Condition E, 190 °C) of 100, 60, and 60 g/10 min, respectively. The sample code (*e.g.*, 15-Na54) indicates the MAA content (15 = 15 wt% MAA) and the neutralization level (Na54 = 54% of the MAA units are neutralized with Na^+). As-received pellets were melt-pressed into 0.2–0.5 mm thick sheets at 140–160 °C in a PHI hot press and quenched to room temperature. The samples were then stored in a desiccator at room temperature for three weeks, unless otherwise indicated. ASTM D1708 dogbones were stamped from these sheets for tensile testing. DMTA samples, cut with a razor blade from the same sheets, had sample dimensions of approximately $5 \times 22\ mm^2$. Specimens of 7–10 mg were also punched from these sheets and placed in aluminum volatile pans for differential scanning calorimetry (DSC).

2.2. Characterization

Uniaxial tensile stress–strain curves were obtained with an Instron Model 5865, equipped with an Environmental Chamber 3111 retrofitted to control the testing temperature to within 0.3 °C with a cycle time of 1 s. Samples were allowed to thermally equilibrate for 5 min prior to testing. Subambient temperatures were achieved by introducing a small quantity of dry ice into the chamber. Results are reported in terms of engineering stress and strain; a constant crosshead separation rate was employed, and the strain rates quoted herein correspond to the initial values. DMTA measurements were performed at 1 Hz on a TA Instruments RSA 3, using the film fixture. Data were collected every 5 °C for an effective heating rate of about 10 °C/min. DSC measurements were run at 10 °C/min on a Perkin–Elmer DSC-7 with type II intracooler, calibrated with indium and tin.

3. Results and discussion

3.1. Yield point determination

Tensile tests of the copolymers [7] and ionomers were performed at various temperatures and strain rates. At sufficiently high strain rates and low temperatures, all copolymers and ionomers showed a local maximum in stress at the yield point. The ionomers, however, retained this local maximum – indicative of necking within the gauge length – to much lower strain rates and higher temperatures. Nevertheless, the degree of necking was not severe; measuring calipers were often needed to verify that necking had taken place.

As in our previous work [7], in order to consistently determine σ_y regardless of the presence or absence of necking, σ_y was taken as the stress exerted on the sample at a strain that corresponds to the intersection of Young's modulus line and a line fit to the pseudo-linear region immediately following the yield point. Fig. 1 depicts this scheme for the $0.38\ s^{-1}$ strain rate tensile test. Our method roughly corresponds to the strain offset method of yield point determination [10], if an offset of 1% is employed. Regardless of composition, strain rate or temperature, the yield strain is consistently 4–6%. Even at the largest strains shown in Fig. 1 (50%), very little *permanent* plastic deformation is observed; after the applied load is removed, almost all of the initial applied strain is recovered over the course of a few days at room temperature. Indeed, it is well known that many ethylene/α-olefin copolymers require strains far beyond this initial yield point to suffer irrecoverable plastic deformation [11]. Recently, Deschanel et al. have considered this recovery to result from stretching and orientation of the entangled amorphous chains, and quantified the importance of this "molecular network contribution" to the measured stress [6]. Consistent with the observation of delayed recovery, this contribution can be quite important at high strains, but it is small at the yield point (*ca.* 5% strain here) and is not considered further in the present work.

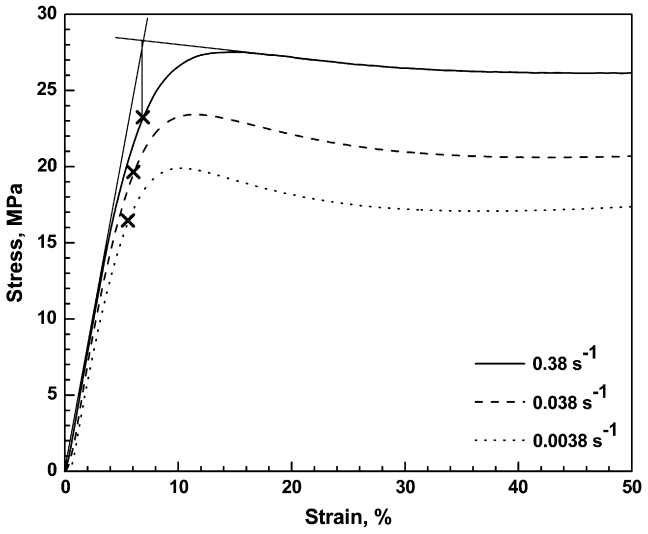

Fig. 1. The yield regime for ionomer 15-Na57, at three different strain rates, all at 25 °C. Young's modulus and post-yield linear fit lines are shown for the $0.38\ s^{-1}$ curve to demonstrate the method for yield point determination. The yield point (×) is shown for all three curves.

3.2. Yield stress model

We have previously formulated a model to describe the origins of the yield stress of the E/MAA copolymers [7]. In short, we sum the contributions to the measured yield stress (σ_y) arising from polyethylene crystal plasticity (σ_c) and incomplete amorphous phase relaxation (σ_{re}):

$$\frac{\sigma_y}{T} = \frac{\sigma_c}{T} + \frac{\sigma_{re}}{T} \tag{1}$$

Following Shadrake and Guiu [12,13], the minimum tensile stress (σ_c) necessary for crystal plasticity via an ($hk0$)[001] slip system is,

$$\sigma_c = \frac{K(T)B}{\pi r_0} \exp\left[\frac{-2\pi\Delta G^*(\dot{\varepsilon})}{K(T)B^2 l_c} - 1\right] \tag{2}$$

where $K(T)$ is the temperature-dependent shear modulus of the slip plane, for which we employed the simulation results of Karasawa et al. [14], B is the magnitude of the Burgers vector equal to the polyethylene crystal c-axis dimension [15] of 0.254 nm, r_0 is the dislocation core radius of 1.0 nm [16], l_c is the crystal thickness, and $G^*(\dot{\varepsilon})$ is the strain rate-dependent energy barrier for the nucleation event [7]. The stress contribution from crystal slip dominates at low strain rates, where the amorphous phase is compliant and its contribution to the observed yield stress is negligible. When the strain rate is large enough, however, the contribution from incomplete amorphous phase relaxation can no longer be ignored. The contribution from each relaxation process may be represented as a term in the Ree–Eyring model [17],

$$\frac{\sigma_{re}}{T} = \sum_i \frac{R}{v_i} \sinh^{-1}\left[\frac{\dot{\varepsilon}}{\dot{\varepsilon}_{o,i}} \exp\left(\frac{\Delta H_i}{RT}\right)\right] \tag{3}$$

where R is the gas constant, v_i is the activation volume, $\dot{\varepsilon}_{0,i}$ is a constant pre-exponential factor and ΔH_i is the activation energy. Fig. 2 illustrates how a system that follows Eq. (1) breaks down into

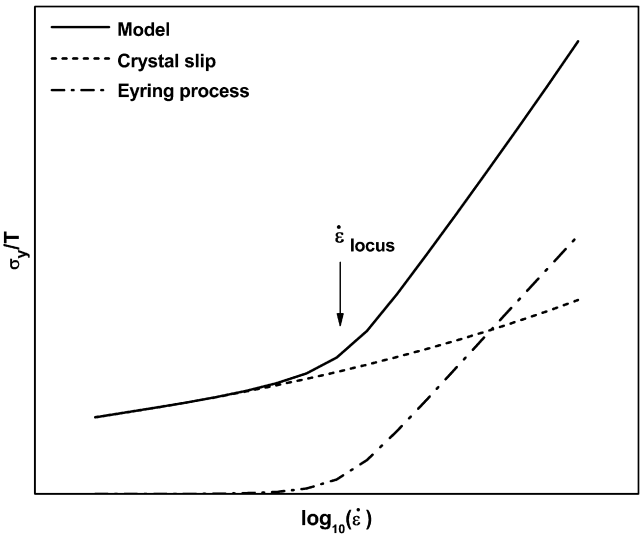

Fig. 2. Schematic showing the relative contributions from rate-dependent crystal slip and a single Eyring process, combined into a single model as described in the text.

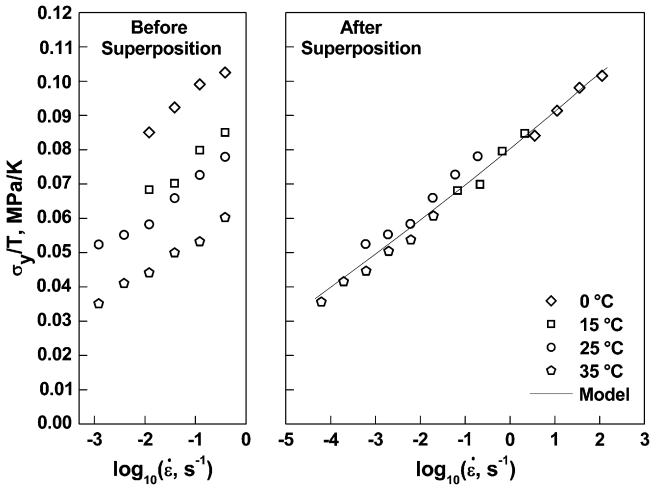

Fig. 3. Left: yield stress for 15-Na57 at various strain rates, at the temperatures indicated. Right: master curve formed from the data via the shift factors given by Eqs. (4)–(6), with the best-fit parameter values in Table 1. Solid line shows the calculated model fit according to Eq. (1).

its respective parts, assuming that only one Eyring process is needed (*i.e.*, $i = 1$ in Eq. (3)). When σ_{re}/T is plotted against the logarithm of $\dot{\varepsilon}$, the regime in which a given relaxation mode is incomplete on the time scale of the experiment shows as a straight line with a slope steeper than that of the crystal slip regime.

3.3. Strain rate–temperature superposition

Superposition of yield stress data in order to form a master curve is an extremely useful tool when comparing yield behavior of various materials. This approach, described in greater detail elsewhere [7], requires both horizontal and vertical shift factors, s_x and s_y, which are coupled as:

$$s_x = \frac{-\Delta H}{R}\left(\frac{1}{T_{ref}} - \frac{1}{T}\right) \tag{4}$$

$$s_y = \frac{\sigma_c\left(T_{ref}, \dot{\varepsilon}_{locus,T_{ref}}\right)}{T_{ref}} - \frac{\sigma_c\left(T, \dot{\varepsilon}_{locus,T}\right)}{T} \tag{5}$$

where,

$$\dot{\varepsilon}_{locus,T} = \frac{\dot{\varepsilon}_0}{2\exp\left(\frac{\Delta H}{RT}\right)} \tag{6}$$

and T_{ref} is the chosen reference temperature for superposition. Eqs. (4)–(6) contain the material parameters ΔH and $\dot{\varepsilon}_0$, which are obtained by fitting Eq. (1) to the unshifted yield stress data by means of a nonlinear least squares algorithm, minimizing the sum of squared residuals in σ_y/T, as described previously [7].

The superposition process for the 15-Na57 ionomer is demonstrated in Fig. 3. The experimentally-determined yield stress was divided by the absolute temperature and plotted against the logarithm of the strain rate. To prevent melting of the thin secondary crystals [18], care was taken never to exceed 35 °C. The results are shown in the left panel. Unlike the copolymers, which clearly display two asymptotes over the range of strain rates and temperatures examined [7], the ionomer shows one. It appears that the amorphous phase is not completely relaxed except at strain rates lower (or temperatures higher) than those probed herein. Without access to the regime in which the amorphous phase is completely relaxed, it is not possible to directly determine l_c by simply fitting equation Eq. (2) to the data in this regime – a procedure which works quite well for the E/MAA copolymers [7]. Nevertheless, neutralization reduces the primary crystal melting temperature, T_{m1}, only very slightly [9]. Thus, l_c should change little upon neutralization, so for each ionomer, we set the $\sigma_c(\dot{\varepsilon})$ function in Eq. (2) equal to that for the corresponding E/MAA copolymer base resin, as determined previously via a similar yield stress analysis [7].

Eq. (1) was fit to these unshifted data using the Levenberg–Marquardt algorithm, setting T_{ref} for this ionomer – and all other materials examined herein – to be 22 °C (295 K). The resulting best-fit parameters are listed in Table 1, while the results of this shifting operation are shown in the right panel of Fig. 3. The line through the data represents Eq. (1) evaluated over the entire range of $\log_{10}\dot{\varepsilon}$, using the best-fit parameter values. Note that superposition broadens the accessible strain rate range by more than three decades.

The superposition process was repeated for all of the 11.5, 15 and 19 wt% MAA ionomers, with the resulting model fits and best-fit

Table 1
Model best-fit parameter values with 2σ (approximately 95%) confidence intervals. The last column lists the expected location of the upturn in σ_y with strain rate for master curves at $T_{ref} = 22$ °C, calculated with Eq. (6) and the best-fit parameter values below.

Ionomer	Na, wt%	v, nm^3	ΔH, kJ/mol	$\log_{10}\dot{\varepsilon}_0$, s^{-1}	$\log_{10}\dot{\varepsilon}_{locus,22\,°C}$, s^{-1}
11.5-Na0	0	2.7 ± 0.1	226 ± 2	39 ± 4	−1 ± 0.1
11.5-Na29	0.9	4.2 ± 0.3	170 ± 10	26 ± 4	−4 ± 1
11.5-Na39	1.2	5.6 ± 0.7	200 ± 30	30 ± 4	−6 ± 1
11.5-Na62	1.9	5.4 ± 0.6	120 ± 20	14 ± 4	−7 ± 2
11.5-Na83	2.6	8 ± 2	170 ± 40	20 ± 4	−10 ± 3
15-Na0	0	2 ± 1	210 ± 2	35 ± 4	−3 ± 0.3
15-Na24	1.0	3.2 ± 0.6	200 ± 30	30 ± 4	−6 ± 1
15-Na34	1.4	3.6 ± 0.6	170 ± 30	24 ± 4	−7 ± 2
15-Na51	2.0	3.1 ± 0.5	120 ± 30	16 ± 4	−6 ± 2
15-Na57	2.3	3.8 ± 0.5	170 ± 20	23 ± 4	−8 ± 2
19-Na0	0	2.0 ± 0.6	219 ± 2	36 ± 4	−3 ± 0.3
19-Na8	0.4	2.4 ± 0.6	210 ± 50	32 ± 4	−5 ± 1
19-Na22	1.1	2.7 ± 0.6	170 ± 40	24 ± 4	−7 ± 2
19-Na35	1.8	2.6 ± 0.4	140 ± 30	19 ± 4	−7 ± 2
19-Na51	2.6	2.7 ± 0.4	140 ± 20	17 ± 4	−7 ± 2

parameter values shown in Fig. 4 and Table 1, respectively. Unlike the copolymers, E/MAA ionomers do not show an abrupt upturn in σ_y with strain rate within the experimental window, but rather a single (almost linear) regime. In all cases, increasing the MAA content or the fraction of sodium-neutralized MAA groups results in a significant increase in σ_y, especially at intermediate strain rates. Interestingly, the benefit of ionomerization occurs with very little neutralization, as shown by Fig. 5, where increasing the neutralization level above *ca.* 0.4 wt% Na results in little further increase in σ_y. Similar results were found for Young's modulus of E/MAA ionomers [9], where above the critical degree of neutralization of 0.4 wt% Na, Young's modulus (E) was barely affected by further neutralization; even though most of the MAA units are not neutralized at this ion content, the "free" MAA units nevertheless associate with the ionic aggregates, so the structure of the material changes little upon further neutralization [9]. Table 1 reveals that virtually all of the ionomers tested in this study – with exception of the 19-Na8 ionomer – contain >0.4 wt% Na. The similarity in behavior between E and σ_y is not altogether unexpected, as the yield strain does not appear to change significantly with neutralization.

DMTA traces at 1 Hz, shown in Fig. 6, reveal two distinct peaks in tan δ for ionomers neutralized to >0.4 wt% Na, in agreement with previous observations [9,19,20]. It is now commonly agreed that the low-temperature relaxation, occurring near −20 °C at 1 Hz, corresponds to the glass transition of ion-depleted, polyethylene-like domains within the amorphous phase [21–23]. At the temperatures and strain rates probed here, this relaxation occurs readily, so the ion-depleted regions do not contribute to σ_y (through Eq. (3)). The peak in tan δ at high temperatures corresponds – at least in part – to the devitrification of the ion-rich regions, a process that is incomplete for these ionomers, even at the lowest strain rates and highest temperatures examined by tensile testing. It is the inability of the polymer chains in these ion-rich "regions of restricted mobility" [8] to completely relax which leads to the observed increase in σ_y upon neutralization, as captured through σ_{re} in Eq. (3). Melting of the thin, secondary polyethylene crystals also contributes to the high-temperature tan δ peak [9]; the presence of the secondary crystals also markedly affects the measured yield stress, as will be discussed in Section 3.4 below.

The best-fit parameter values (Table 1) for the single Eyring process, corresponding to the amorphous phase relaxation, merit some discussion. First, the activation volume, v, appears to increase with neutralization, as shown graphically in Fig. 7. In particular, v for the 11.5 wt% MAA series is a strong function of ion content, with Fig. 7 showing a much higher slope than for the ionomers derived from copolymers containing 15 or 19 wt% MAA. While the reasons

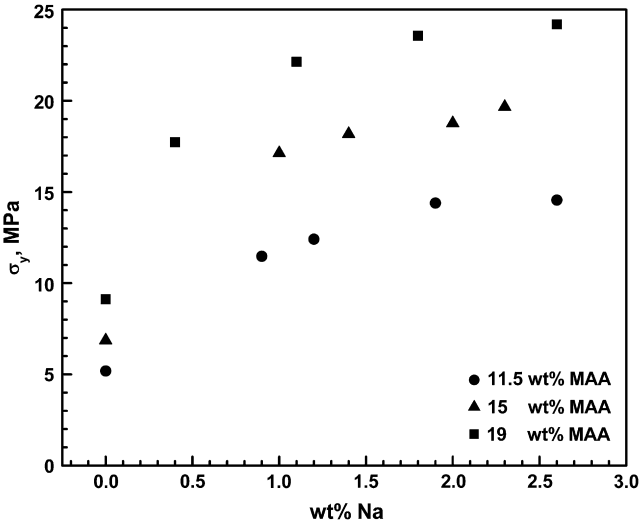

Fig. 5. The effect of increasing ion content for three series of ionomers based on copolymers of different MAA contents. Results are for a temperature of 22 °C and fixed strain rate corresponding to $\log_{10}\dot{\varepsilon} = -1.3$.

underlying these different slopes remain unclear, it may be noteworthy that the high-temperature tan δ peak (Fig. 6) behaves similarly: for the 15 or 19 wt% MAA ionomers, little increase in the tan δ peak temperature is observed above the critical ion content of 0.4 wt% Na, while for the 11.5 wt% MAA ionomers, the tan δ peak temperature increases continuously, even up to 2.5 wt% Na. Second, though the uncertainties associated with the activation energy are large, ΔH appears to decrease with neutralization, with values ranging between 120 and 230 kJ/mol. Tachino et al. [21] reported values of 300–400 kJ/mol for the activation energy of the high-temperature (α) relaxation observed dielectrically in sodium-neutralized ionomers based on a 15 wt% MAA copolymer, about twice what we find here. However, such dielectric measurements are complicated by the melting of both primary and secondary crystals, which overlap in temperature with the α relaxation at the relatively high frequencies employed for dielectric spectroscopy. Finally, even though the crystal slip regime is not accessed experimentally, we have set σ_c for each ionomer (Eq. (1)) equal to that for its parent copolymer, so the crossover strain rate $\dot{\varepsilon}_{\mathrm{locus},T_{\mathrm{ref}}}$ – the point at which incomplete amorphous phase relaxation starts to contribute significantly to the yield stress at T_{ref}—can nevertheless be calculated from Eq. (6) and the best-fit values of $\dot{\varepsilon}_0$ and ΔH. The results are listed in Table 1. When the neutralization level is above

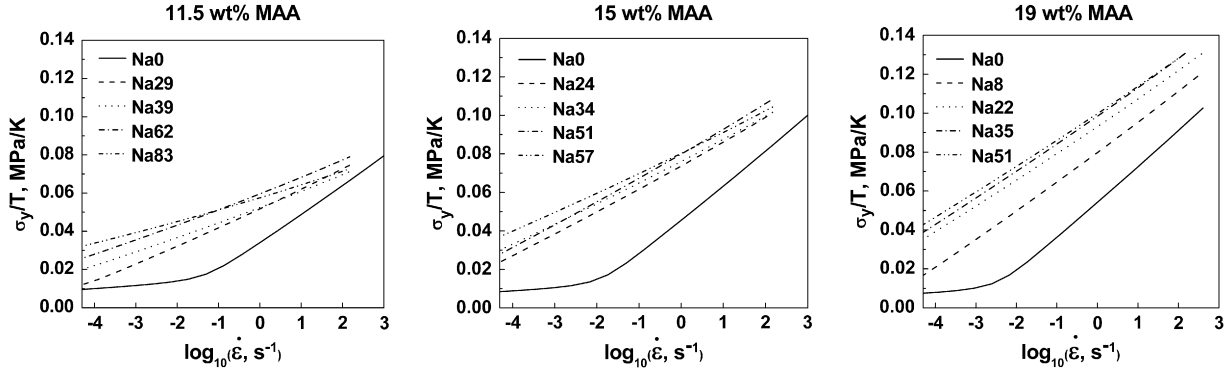

Fig. 4. Comparison of master curves as a function of MAA content and degree of neutralization, all with $T_{\mathrm{ref}} = 22$ °C. Data points are omitted to preserve legibility, but the horizontal extent of each curve corresponds to the actual range of $\log_{10}\dot{\varepsilon}$ spanned.

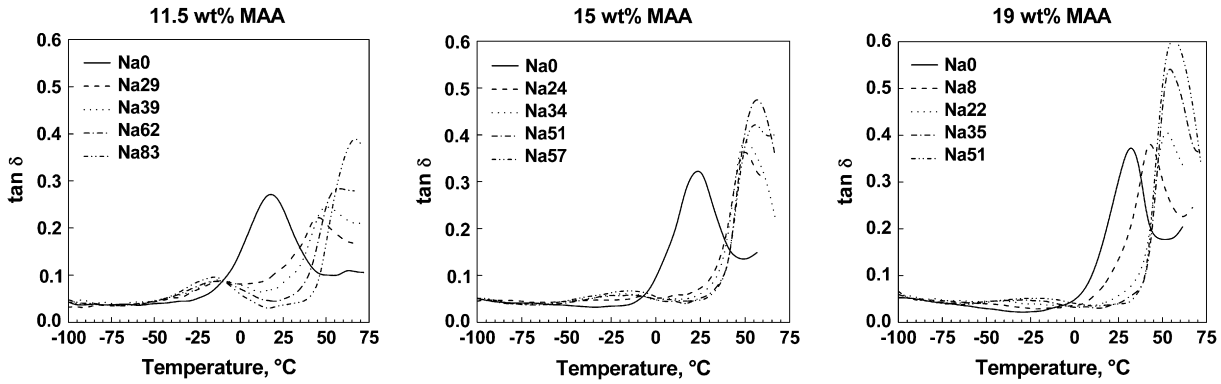

Fig. 6. DMTA data at 1 Hz for E/MAA copolymers and ionomers. E/MAA copolymers display a single β relaxation over this range of temperature. Partial neutralization results in a split of this peak into two relaxations.

0.4 wt% Na, the crossover occurs at a very low strain rate (typically $10^{-7}\ s^{-1}$), especially as compared to the copolymers (typically $10^{-2}\ s^{-1}$). The 19-Na8 ionomer – the only one with ion content near the critical degree of neutralization – shows the crossover at an intermediate value of strain rate ($10^{-5}\ s^{-1}$).

Fig. 4 shows that σ_y for the E/MAA copolymers and ionomers approaches each other at high strain rates. In this regime, the copolymer amorphous phase is glassy [7] and the ionomer regions of restricted mobility are stiff; for both materials, the amorphous phase is not compliant. However, at even higher strain rates – above those measured in this study – the ion-poor regions within the ionomer amorphous phase will also be incapable of relaxation on the time scale of a standard tensile test and will make an additional contribution to σ_{re} in Eq. (3). We expect that this will lead to yet another upturn in the ionomer yield stress at high strain rates, corresponding to an additional process with an activation volume v similar to that found for the copolymers (2 nm^3); in other words, we expect that the σ_y curves for the ionomers should shift to parallel those for the copolymers in Fig. 4, rather than crossing them. Dielectric spectroscopy of the low-temperature (β) relaxation in an 11-Na53 ionomer [20] implies that, at 22 °C, the ion-poor regions will vitrify at $\log_{10}\dot{\varepsilon} = 3$—4, slightly beyond the range accessed in our experiments (Fig. 4) but quite relevant for the rates experienced in impact testing.

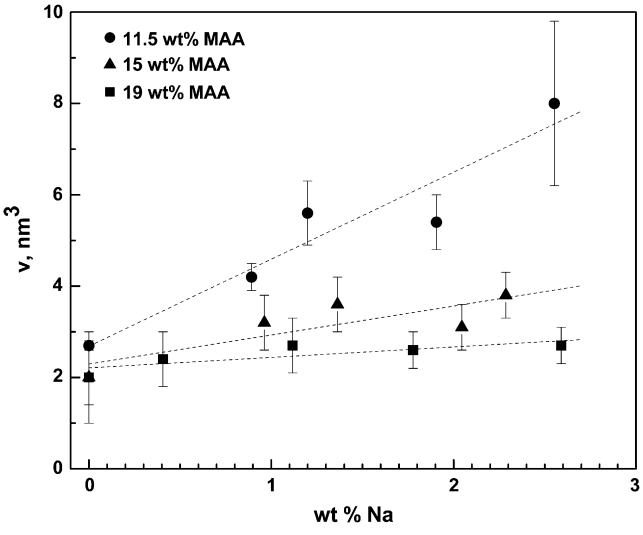

Fig. 7. Change in activation volume with ion content.

3.4. Implications of secondary crystallization

It is well known that thin secondary crystals form slowly in these materials during room temperature annealing [18]. This is reflected by the growth of a secondary melting endotherm which also moves to higher temperatures with annealing time. The time evolution of the DSC traces for 19-Na51 is shown in Fig. 8 inset as an example; based on the total area of the melting endotherms, the crystalline weight fraction of this ionomer increases from 0.08 to 0.13 after five days at room temperature. For the parent E/MAA copolymer (19-Na0), the yield stress measured at a typical laboratory test rate ($\log_{10}\dot{\varepsilon} = -1.3$) increases slightly over this same time interval, as shown in Fig. 8. We attribute this modest increase to a small elevation of the amorphous-phase T_g, as the low-T_g ethylene segments are selectively removed via crystallization; this small increase in T_g thereby increases σ_{re}, which is substantial even for the copolymers at ($\log_{10}\dot{\varepsilon} = -1.3$) (see Fig. 4).

The ionomers, on the other hand, show a far more drastic increase in σ_y with aging time. Fig. 8 shows that σ_y for 19-Na51

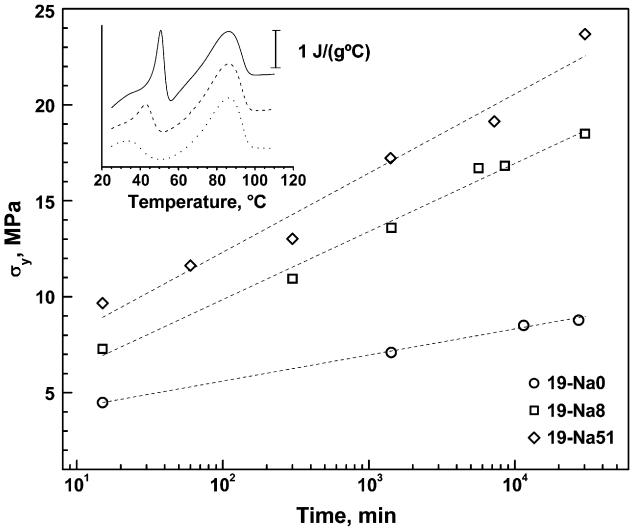

Fig. 8. Change in the measured yield stress σ_y, at 25 °C and $\log_{10}\dot{\varepsilon} = -1.3$, with room-temperature annealing time for E/19MAA copolymer and ionomers. The inset shows the growth of the secondary crystal melting endotherm for a 19-Na51 ionomer with room-temperature annealing time following quenching of the melt to room temperature: (···) 15 min, (- -) 5 h, and (—) 5 days.

increases by about 14 MPa, roughly 5× the change for the parent copolymer. In the ionomers, these thin secondary crystals serve to bridge the stiff regions of restricted mobility surrounding the ionic aggregates [9], thereby enhancing the continuity of the "hard" regions within the amorphous phase and increasing σ_y. These changes in continuity are not adequately captured by the simple series sum in Eq. (1), which further underscores the importance of understanding the complicated interplay of the microstructural elements within E/MAA ionomers.

4. Conclusions

Partial neutralization greatly increases the yield stress of E/MAA ionomers at typical laboratory strain rates. A model incorporating contributions from polyethylene crystal slip and relaxation of the amorphous phase, previously developed for and applied to the rate dependence of the yield stress of nonionic E/MAA copolymers [7], gives a satisfactory description of the rate dependence for the ionomers as well, allowing yield stress data taken over a range of temperatures to be superposed. Compared with the E/MAA copolymers, neutralization strongly shifts the amorphous-phase process to lower rates, even at modest ion contents; most of the effect of neutralization is captured when 0.4 wt% Na is reached. The slowdown of amorphous phase relaxation results from the formation of ionic aggregates and the "regions of restricted mobility" which surround them, which relax much more slowly than the amorphous phase in the nonionic copolymer, as also observed by dynamic mechanical thermal analysis. Finally, the changes in the yield stress with room temperature annealing were considered. The thin secondary polyethylene crystals that form over time progressively and substantially raise the yield stress, as they effectively bridge the regions of restricted mobility, creating a sample-spanning rigid pathway which requires greater stress to plastically deform.

Acknowledgements

This work was generously supported by DuPont Packaging and Industrial Polymers, Sabine River Works. The authors thank Dr. George Prejean of DuPont for providing some of the materials studied herein, and for helpful discussions throughout.

References

[1] Eisenberg A, Kim J-S. Introduction to ionomers. New York: John Wiley & Sons, Inc.; 1998. p. 2.
[2] Akimoto HA, Kanazawa T, Yamada M, Matsuda S, Shonaike GO, Murakami A. J Appl Polym Sci 2001;81:1712–20.
[3] Longworth R, Nagel H. Packaging. In: Tant MR, Mauritz KA, Wilkes GL, editors. Ionomers: synthesis, structure, properties and applications. London: Blackie Academic & Professional; 1997. p. 365.
[4] Rees RW, Vaughan DJ. Polym Prepr (Am Chem Soc Div Polym Chem) 1965;6:296–303.
[5] Hirasawa E, Yamamoto Y, Tadano K, Yano S. J Appl Polym Sci 1991;42:351–62.
[6] Deschanel S, Greviskes BP, Bertoldi K, Sarva SS, Chen W, Samuels SL, et al. Polymer 2008;50:227–35.
[7] Scogna RC, Register RA. Polymer 2008;49:992–8.
[8] Eisenberg A, Hird B, Moore RB. Macromolecules 1990;23:4098–107.
[9] Wakabayashi K, Register RA. Macromolecules 2006;39:1079–86.
[10] Ward IM. Mechanical properties of solid polymers. 2nd ed. Chichester, Sussex; New York: Wiley; 1983.
[11] Hiss R, Hobeika S, Lynn C, Strobl G. Macromolecules 1999;32:4390–403.
[12] Shadrake LG, Guiu F. Philos Mag 1976;34:565–81.
[13] Shadrake LG, Guiu F. Philos Mag A 1979;39:785–96.
[14] Karasawa N, Dasgupta S, Goddard WA. J Phys Chem 1991;95:2260–72.
[15] Crist B. Plastic deformation of polymers. In: Cahn RW, Haasen P, Kramer EJ, editors. Materials science and technology: a comprehensive treatment. New York: VCH Publishers Inc.; 1993. p. 427–69.
[16] Bacon DJ, Tharmalingham K. J Mater Sci 1983;18:884–93.
[17] Ree T, Eyring H. J Appl Phys 1955;26:793–800.
[18] Loo Y-L, Wakabayashi K, Huang YE, Register RA, Hsiao BS. Polymer 2005;46:5118–24.
[19] MacKnight WJ, McKenna LW, Read BE. J Appl Phys 1967;38:4208–12.
[20] Read BE, Carter EA, Connor TM, MacKnight WJ. Br Polym J 1969;1:123–31.
[21] Tachino H, Hara H, Hirasawa E, Kutsumizu S, Tadano K, Yano S. Macromolecules 1993;26:752–7.
[22] Khanna YP, Wenner WM, Krutzel L. Macromolecules 1988;21:268–70.
[23] MacKnight WJ, Earnest Jr TR. J Polym Sci D Macromol Rev 1981;16:41–122.